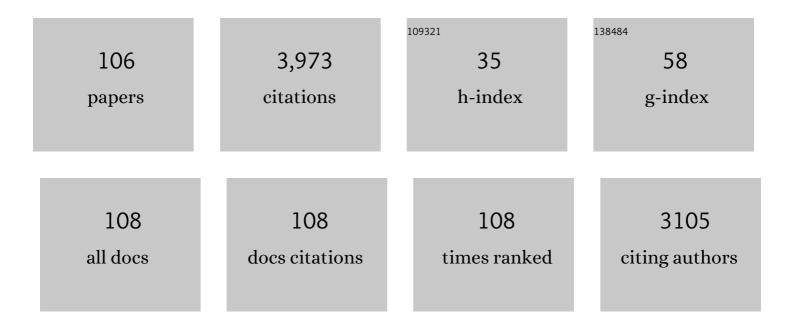
Zhi-Xiang Wang

List of Publications by Year in descending order

Source: https://exaly.com/author-pdf/390218/publications.pdf Version: 2024-02-01



#	Article	IF	CITATIONS
1	Semi-interpenetrating-network all-solid-state polymer electrolyte with liquid crystal constructing efficient ion transport channels for flexible solid lithium-metal batteries. Journal of Energy Chemistry, 2022, 67, 157-167.	12.9	23
2	Pyrylium salts acting as both energy transfer and electron transfer photocatalysts for <i>E</i> → <i>Z</i> isomerization of activated alkenes and cyclization of cinnamic or biaryl carboxylic acids. Organic Chemistry Frontiers, 2022, 9, 973-978.	4.5	7
3	Visible-light-induced N-heterocyclic carbene mediated cascade transformation of N-alkenoxypyridinium salts. Chinese Chemical Letters, 2022, 33, 4298-4302.	9.0	13
4	Alkynyl Sulfonium Salts Can Be Employed as Chalcogenâ€Bonding Catalysts and Generate Alkynyl Radicals under Blue‣ight Irradiation. Angewandte Chemie - International Edition, 2022, 61, .	13.8	36
5	Alkynyl Sulfonium Salts Can Be Employed as Chalcogenâ€Bonding Catalysts and Generate Alkynyl Radicals under Blueâ€Light Irradiation. Angewandte Chemie, 2022, 134, .	2.0	8
6	DFT insight into asymmetric alkyl–alkyl bond formation <i>via</i> nickel-catalysed enantioconvergent reductive coupling of racemic electrophiles with olefins. Chemical Science, 2022, 13, 3728-3739.	7.4	9
7	DFT Mechanistic Insights into Aldehyde Deformylations with Biomimetic Metal–Dioxygen Complexes: Distinct Mechanisms and Reaction Rules. Jacs Au, 2022, 2, 745-761.	7.9	6
8	Innentitelbild: Alkynyl Sulfonium Salts Can Be Employed as Chalcogenâ€Bonding Catalysts and Generate Alkynyl Radicals under Blueâ€Light Irradiation (Angew. Chem. 16/2022). Angewandte Chemie, 2022, 134, .	2.0	0
9	Divergent isoindolinone synthesis through palladium-catalyzed isocyanide bridging C–H activation. Cell Reports Physical Science, 2022, 3, 100776.	5.6	9
10	N-Heterocyclic Nitreniums Can Be Employed as Photoredox Catalysts for the Single-Electron Reduction of Aryl Halides. Organic Letters, 2022, 24, 4598-4602.	4.6	16
11	Z â€Selective αâ€Arylation of α,βâ€Unsaturated Nitriles via [3,3]â€Sigmatropic Rearrangement. Angewandte C 2021, 133, 2369-2375.	hemie, 2.0	4
12	<i>Z</i> â€Selective αâ€Arylation of α,βâ€Unsaturated Nitriles via [3,3]â€Sigmatropic Rearrangement. Angewar Chemie - International Edition, 2021, 60, 2339-2345.	ndte 13.8	21
13	Photoinduced α-Alkenylation of Katritzky Salts: Synthesis of β,γ-Unsaturated Esters. Organic Letters, 2021, 23, 1577-1581.	4.6	22
14	System: A DFT Mechanistic Study. Organic Letters, 2021, 23, 1535-1540.	4.6	15
15	Morita–Baylis–Hillmanâ€Type [3,3]â€Rearrangement: Switching from <i>Z</i> ―to <i>E</i> â€Selective αâ€ by New Rearrangement Partners. Angewandte Chemie - International Edition, 2021, 60, 11414-11422.	Arylation	10
16	Morita–Baylis–Hillmanâ€Type [3,3]â€Rearrangement: Switching from Z ―to E â€Selective αâ€Arylation by Rearrangement Partners. Angewandte Chemie, 2021, 133, 11515-11523.	New 2.0	2
17	Donor–Acceptor Complex Enables Cascade Radical Cyclization of <i>N</i> -Arylacrylamides with Katritzky Salts. Organic Letters, 2021, 23, 5425-5429.	4.6	15
18	Visible‣ightâ€Induced Selective Photolysis of Phosphonium Iodide Salts for Monofluoromethylations. Angewandte Chemie - International Edition, 2021, 60, 25477-25484.	13.8	69

#	Article	IF	CITATIONS
19	Visible‣ightâ€Induced Selective Photolysis of Phosphonium Iodide Salts for Monofluoromethylations. Angewandte Chemie, 2021, 133, 25681-25688.	2.0	8
20	α-C–H difluoroalkylation of alkyl sulfoxides <i>via</i> intermolecular Pummerer reaction. Organic Chemistry Frontiers, 2021, 8, 1280-1287.	4.5	5
21	A donor–acceptor complex enables the synthesis of <i>E</i> -olefins from alcohols, amines and carboxylic acids. Chemical Science, 2021, 12, 6684-6690.	7.4	22
22	Additive-Free, Visible-Light-Enabled Decarboxylative Alkylation of Enamides. Organic Letters, 2021, 23, 8262-8266.	4.6	21
23	DFT Mechanistic Account for the Site Selectivity of Electron-Rich C(sp ³)–H Bond in the Manganese-Catalyzed Aminations. Organic Letters, 2020, 22, 453-457.	4.6	25
24	Photochemical Decarboxylative C(sp ³)–X Coupling Facilitated by Weak Interaction of N-Heterocyclic Carbene. Organic Letters, 2020, 22, 8059-8064.	4.6	30
25	Highly enantioselective 1,6-addition of dienolates to coumarins and chromones through N-heterocyclic carbene catalysis. Organic Chemistry Frontiers, 2020, 7, 3692-3697.	4.5	8
26	How does the nickel catalyst control the doubly enantioconvergent coupling of racemic alkyl nucleophiles and electrophiles? The rebound mechanism. Organic Chemistry Frontiers, 2020, 7, 3411-3419.	4.5	8
27	Visible-Light-Triggered Iodinations Facilitated by Weak Electrostatic Interaction of N-Heterocyclic Carbenes. Organic Letters, 2020, 22, 7187-7192.	4.6	26
28	Red-emissive poly(phenylene vinylene)-derivated semiconductors with well-balanced ambipolar electrical transporting properties. Journal of Materials Chemistry C, 2020, 8, 10868-10879.	5.5	18
29	Density Functional Theory Mechanistic Study of Ni-Catalyzed Reductive Alkyne–Alkyne Cyclodimerization: Oxidative Cyclization versus Outer-Sphere Proton Transfer. Organic Letters, 2020, 22, 2454-2459.	4.6	18
30	Understanding the Chemoselectivity in Palladium-Catalyzed Three-Component Reaction of <i>o</i> -Bromobenzaldehyde, <i>N</i> -Tosylhydrazone, and Methanol. Organic Letters, 2020, 22, 3251-3257.	4.6	15
31	Asymmetric Iodonio-[3,3]-Sigmatropic Rearrangement to Access Chiral α-Aryl Carbonyl Compounds. Journal of the American Chemical Society, 2020, 142, 6884-6890.	13.7	32
32	Site-Selective Pyridyl Alkyl Ketone Synthesis from <i>N</i> -Alkenoxypyridiniums through Boekelheide-Type Rearrangements. Organic Letters, 2020, 22, 5617-5621.	4.6	13
33	Palladium-Catalyzed Three-Component Coupling Reaction of <i>o</i> -Bromobenzaldehyde, <i>N</i> -Tosylhydrazone, and Methanol. Organic Letters, 2020, 22, 2087-2092.	4.6	25
34	DFT Mechanistic Insight into the Dioxygenase-like Reactivity of a Co ^{III} -peroxo Complex: O–O Bond Cleavage via a [1,3]-Sigmatropic Rearrangement-like Mechanism. Inorganic Chemistry, 2020, 59, 2051-2061.	4.0	8
35	DFT Study of PNP-Mn-Catalyzed Acceptorless Dehydrogenative Coupling of Primary Alcohols with Hydrazine to Give Alkene or Azine. Organometallics, 2019, 38, 3590-3601.	2.3	6
36	Density Functional Theory Mechanistic Insight into the Base-Free Nickel-Catalyzed Suzuki–Miyaura Cross-Coupling of Acid Fluoride: Concerted versus Stepwise Transmetalation. Journal of Organic Chemistry, 2019, 84, 13983-13991.	3.2	24

#	Article	IF	CITATIONS
37	The <i>ortho</i> â€Difluoroalkylation of Aryliodanes with Enol Silyl Ethers: Rearrangement Enabled by a Fluorine Effect. Angewandte Chemie, 2019, 131, 6017-6022.	2.0	15
38	The <i>ortho</i> â€Difluoroalkylation of Aryliodanes with Enol Silyl Ethers: Rearrangement Enabled by a Fluorine Effect. Angewandte Chemie - International Edition, 2019, 58, 5956-5961.	13.8	75
39	Selective [5,5]‣igmatropic Rearrangement by Assembly of Aryl Sulfoxides with Allyl Nitriles. Angewandte Chemie - International Edition, 2019, 58, 5316-5320.	13.8	47
40	Selective [5,5]‣igmatropic Rearrangement by Assembly of Aryl Sulfoxides with Allyl Nitriles. Angewandte Chemie, 2019, 131, 5370-5374.	2.0	14
41	Gold-Catalyzed Atom-Economic Synthesis of Sulfone-Containing Pyrrolo[2,1- <i>a</i>]isoquinolines from Diynamides: Evidence for Consecutive Sulfonyl Migration. ACS Catalysis, 2019, 9, 2610-2617.	11.2	49
42	A Unified Mechanism to Account for Manganese―or Rutheniumâ€Catalyzed Nitrile αâ€Olefinations by Primary or Secondary Alcohols: A DFT Mechanistic Study. Chemistry - A European Journal, 2019, 25, 3939-3949.	3.3	14
43	Computational mechanistic study of Ru-catalyzed CO ₂ reduction by pinacolborane revealing the σ–Ĩ€ coupling mechanism for CO ₂ decarbonylation. Dalton Transactions, 2018, 47, 4804-4819.	3.3	6
44	Reductive <i>ortho</i> C–H cyanoalkylation of aryl(heteroaryl) sulfoxides: a general approach to α-aryl(heteroaryl) nitriles. Organic Chemistry Frontiers, 2018, 5, 1756-1762.	4.5	25
45	Viable aromatic Be _n H _n stars enclosing a planar hypercoordinate boron or late transition metal. Physical Chemistry Chemical Physics, 2018, 20, 7217-7222.	2.8	21
46	Strong Preference of the Redoxâ€Neutral Mechanism over the Redox Mechanism for the Ti ^{IV} Catalysis Involved in the Carboamination of Alkyne with Alkene and Diazene. Chemistry - A European Journal, 2018, 24, 7010-7025.	3.3	12
47	Palladium-Catalyzed Reductive Cross-Coupling Reaction of Aryl Chromium(0) Fischer Carbene Complexes with Aryl Iodides. Organometallics, 2018, 37, 1-10.	2.3	24
48	A Pseudodearomatized PN ³ P*Ni–H Complex as a Ligand and σ-Nucleophilic Catalyst. Journal of Organic Chemistry, 2018, 83, 14969-14977.	3.2	21
49	A comparative DFT study of TBD-catalyzed reactions of amines with CO ₂ and hydrosilane: the effect of solvent polarity on the mechanistic preference and the origins of chemoselectivities. Chemical Communications, 2018, 54, 10870-10873.	4.1	25
50	Selective <i>ortho</i> Câ^'H Cyanoalkylation of (Diacetoxyiodo)arenes through [3,3]‣igmatropic Rearrangement. Angewandte Chemie, 2018, 130, 9216-9220.	2.0	22
51	Selective <i>ortho</i> Câ^H Cyanoalkylation of (Diacetoxyiodo)arenes through [3,3]‣igmatropic Rearrangement. Angewandte Chemie - International Edition, 2018, 57, 9078-9082.	13.8	47
52	A strategy for developing metal-free hydrogenation catalysts: a DFT proof-of-principle study. Dalton Transactions, 2018, 47, 7709-7714.	3.3	4
53	Diverse catalytic reactivity of a dearomatized PN ³ P*–nickel hydride pincer complex towards CO ₂ reduction. Chemical Communications, 2018, 54, 11395-11398.	4.1	56
54	The Origins of the Differences between Alkyne Hydroalkoxylations Catalyzed by 8â€Quinolinolato―and Dipyrrinatoâ€Ligated Rh ^I Complexes: A DFT Mechanistic Study. European Journal of Inorganic Chemistry, 2017, 2017, 2713-2722.	2.0	7

#	Article	IF	CITATIONS
55	Noncovalent Molecular Heterojunction: Structure Determination and Property Characterization using Scanning Tunneling Microscopy/Spectroscopy and Theoretical Calculations. Journal of Physical Chemistry C, 2017, 121, 13701-13706.	3.1	6
56	Zigzag double-chain C–Be nanoribbon featuring planar pentacoordinate carbons and ribbon aromaticity. Journal of Materials Chemistry C, 2017, 5, 408-414.	5.5	10
57	Differences between the elimination of early and late transition metals: DFT mechanistic insights into the titanium-catalyzed synthesis of pyrroles from alkynes and diazenes. Chemical Science, 2017, 8, 2413-2425.	7.4	27
58	A DFT study unveils the secret of how H ₂ is activated in the N-formylation of amines with CO ₂ and H ₂ catalyzed by Ru(<scp>ii</scp>) pincer complexes in the absence of exogenous additives. Chemical Communications, 2017, 53, 12148-12151.	4.1	18
59	Formylation or methylation: what determines the chemoselectivity of the reaction of amine, CO ₂ , and hydrosilane catalyzed by 1,3,2-diazaphospholene?. Chemical Science, 2017, 8, 7637-7650.	7.4	28
60	Linear, planar, and tubular molecular structures constructed by double planar tetracoordinate carbon <i>D</i> ₂ <i>_h</i> C ₂ (BeH) ₄ species via hydrogenâ€bridged BeH ₂ Be bonds. Journal of Computational Chemistry, 2016, 37, 261-269.	3.3	14
61	Metal-free homolytic hydrogen activation: a quest through density functional theory computations. New Journal of Chemistry, 2016, 40, 8141-8148.	2.8	6
62	How Does an Earth-Abundant Copper-Based Catalyst Achieve Anti-Markovnikov Hydrobromination of Alkynes? A DFT Mechanistic Study. Organometallics, 2016, 35, 1923-1930.	2.3	16
63	Unveiling Secrets of Overcoming the "Heteroatom Problem―in Palladium-Catalyzed Aerobic C–H Functionalization of Heterocycles: A DFT Mechanistic Study. Journal of the American Chemical Society, 2016, 138, 2712-2723.	13.7	65
64	Four Decades of the Chemistry of Planar Hypercoordinate Compounds. Angewandte Chemie - International Edition, 2015, 54, 9468-9501.	13.8	217
65	Mechanistic Insight into Ketone α-Alkylation with Unactivated Olefins via C–H Activation Promoted by Metal–Organic Cooperative Catalysis (MOCC): Enriching the MOCC Chemistry. Journal of the American Chemical Society, 2015, 137, 6279-6291.	13.7	66
66	Palladium-Catalyzed C–H Functionalization of Acyldiazomethane and Tandem Cross-Coupling Reactions. Journal of the American Chemical Society, 2015, 137, 4435-4444.	13.7	94
67	DFT mechanistic study of the H ₂ -assisted chain transfer copolymerization of propylene and <i>p</i> -methylstyrene catalyzed by zirconocene complex. Journal of Polymer Science Part A, 2015, 53, 576-585.	2.3	10
68	Depolymerization of Oxidized Lignin Catalyzed by Formic Acid Exploits an Unconventional Elimination Mechanism Involving 3c–4e Bonding: A DFT Mechanistic Study. ACS Catalysis, 2015, 5, 6386-6396.	11.2	46
69	Assessing the performance of commonly used DFT functionals in studying the chemistry of frustrated Lewis pairs. Journal of Theoretical and Computational Chemistry, 2014, 13, 1350074.	1.8	21
70	D3h [A-CE3-A]â^' (E = Al and Ga, A = Si, Ge, Sn, and Pb): A new class of hexatomic mono-anionic species with trigonal bipyramidal carbon. Journal of Chemical Physics, 2014, 140, 104302.	3.0	5
71	Gold catalyzed hydrogenations of small imines and nitriles: enhanced reactivity of Au surface toward H ₂ via collaboration with a Lewis base. Chemical Science, 2014, 5, 1082-1090.	7.4	91
72	Computational Mechanistic Study of Fe-Catalyzed Hydrogenation of Esters to Alcohols: Improving Catalysis by Accelerating Precatalyst Activation with a Lewis Base. ACS Catalysis, 2014, 4, 4377-4388.	11.2	91

#	Article	IF	CITATIONS
73	Hydrogenation of Esters Catalyzed by Ruthenium PN ³ -Pincer Complexes Containing an Aminophosphine Arm. Organometallics, 2014, 33, 4152-4155.	2.3	74
74	Mechanism of <i>Z</i> -Selective Olefin Metathesis Catalyzed by a Ruthenium Monothiolate Carbene Complex: A DFT Study. Organometallics, 2014, 33, 4290-4294.	2.3	20
75	How accurate are the popular PCM/GB continuum solvation models for calculating the solvation energies of amino acid side-chain analogs?. Theoretical Chemistry Accounts, 2014, 133, 1.	1.4	14
76	A Computational Mechanistic Study of an Unprecedented Heck-Type Relay Reaction: Insight into the Origins of Regio- and Enantioselectivities. Journal of the American Chemical Society, 2014, 136, 986-998.	13.7	118
77	Catalytic Mechanisms of Direct Pyrrole Synthesis via Dehydrogenative Coupling Mediated by PNP-Ir or PNN-Ru Pincer Complexes: Crucial Role of Proton-Transfer Shuttles in the PNP-Ir System. Journal of the American Chemical Society, 2014, 136, 4974-4991.	13.7	171
78	Mechanism of the Methyltrioxorheniumâ€Catalyzed Deoxydehydration of Polyols: A New Pathway Revealed. Chemistry - A European Journal, 2013, 19, 3827-3832.	3.3	71
79	Density Functional Theory Mechanistic Study of the Reduction of CO ₂ to CH ₄ Catalyzed by an Ammonium Hydridoborate Ion Pair: CO ₂ Activation via Formation of a Formic Acid Entity. Inorganic Chemistry, 2013, 52, 12098-12107.	4.0	65
80	Mechanism and Origins of <i>Z</i> Selectivity of the Catalytic Hydroalkoxylation of Alkynes via Rhodium Vinylidene Complexes To Produce Enol Ethers. Organometallics, 2013, 32, 2804-2813.	2.3	26
81	Differences between insertions of ethylene into metallocene and nonâ€metallocene ethylene polymerization catalysts. Journal of Physical Organic Chemistry, 2013, 26, 70-76.	1.9	4
82	Manipulation of the Reducibility of Ceria‣upported Au Catalysts by Interface Engineering. ChemCatChem, 2013, 5, 1308-1312.	3.7	11
83	D3h CN3Be3+ and CO3Li3+: viable planar hexacoordinate carbon prototypes. Physical Chemistry Chemical Physics, 2012, 14, 14760.	2.8	59
84	Catalytic metal-free intramolecular hydroaminations of non-activated aminoalkenes: A computational exploration. Dalton Transactions, 2012, 41, 9091.	3.3	23
85	Computational Insight into the Mechanism of Selective Imine Formation from Alcohol and Amine Catalyzed by the Ruthenium(II)â€₽NP Pincer Complex. European Journal of Inorganic Chemistry, 2012, 2012, 5011-5020.	2.0	79
86	Computational Design of Metal-Free Molecules for Activation of Small Molecules, Hydrogenation, and Hydroamination. Topics in Current Chemistry, 2012, 332, 231-266.	4.0	8
87	Does the Ruthenium Nitrato Catalyst Work Differently in <i>Z</i> -Selective Olefin Metathesis? A DFT Study. Organometallics, 2012, 31, 8654-8657.	2.3	52
88	A Thorough DFT Study of the Mechanism of Homodimerization of Terminal Olefins through Metathesis with a Chelated Ruthenium Catalyst: From Initiation to <i>Z</i> Selectivity to Regeneration. Organometallics, 2012, 31, 7222-7234.	2.3	58
89	Computational mechanistic studies of acceptorless dehydrogenation reactions catalyzed by transition metal complexes. Science China Chemistry, 2012, 55, 1991-2008.	8.2	22
90	Computational Mechanistic Study of the Hydrogenation of Carbonate to Methanol Catalyzed by the Ru ^{II} PNN Complex. Inorganic Chemistry, 2012, 51, 5716-5727.	4.0	77

#	Article	IF	CITATIONS
91	Reaction Mechanism of Phosphaneâ€Catalyzed [4+2] Annulations between αâ€Alkylallenoates and Activated Alkenes: A Computational Study. European Journal of Organic Chemistry, 2012, 2012, 3587-3597.	2.4	45
92	Metal-free catalysts for hydrogenation of both small and large imines: a computational experiment. Dalton Transactions, 2011, 40, 1929.	3.3	25
93	How Does the Nickel Pincer Complex Catalyze the Conversion of CO ₂ to a Methanol Derivative? A Computational Mechanistic Study. Inorganic Chemistry, 2011, 50, 3816-3825.	4.0	159
94	Computational Study on the Catalytic Role of Pincer Ruthenium(II)-PNN Complex in Directly Synthesizing Amide from Alcohol and Amine: The Origin of Selectivity of Amide over Ester and Imine. Organometallics, 2011, 30, 5233-5247.	2.3	149
95	Designing Metalâ€Free Catalysts by Mimicking Transitionâ€Metal Pincer Templates. Chemistry - A European Journal, 2011, 17, 2038-2043.	3.3	34
96	Insight into the relative reactivity of "Frustrated Lewis pairs―and stable carbenes in activating H2 and CH4: A comparative computational study. Physical Chemistry Chemical Physics, 2010, 12, 5268.	2.8	44
97	Encumbering the intramolecular ï€ donation by using a bridge: A strategy for designing metal-free compounds to hydrogen activation. Science Bulletin, 2010, 55, 239-245.	1.7	38
98	Reversible Heterolytic Methane Activation of Metalâ€Free Closedâ€Shell Molecules: A Computational Proofâ€ofâ€Principle Study. European Journal of Inorganic Chemistry, 2010, 2010, 2254-2260.	2.0	35
99	Computationally Designed Families of Flat, Tubular, and Cage Molecules Assembled with "Starbenzene― Building Blocks through Hydrogenâ€Bridge Bonds. Chemistry - A European Journal, 2010, 16, 1271-1280.	3.3	38
100	The Catalytic Role of N-Heterocyclic Carbene in a Metal-Free Conversion of Carbon Dioxide into Methanol: A Computational Mechanism Study. Journal of the American Chemical Society, 2010, 132, 12388-12396.	13.7	235
101	Computationally Designed Metal-Free Hydrogen Activation Site: Reaching the Reactivity of Metalâ ^{~?} Ligand Bifunctional Hydrogenation Catalysts. Inorganic Chemistry, 2010, 49, 295-301.	4.0	61
102	CAl4Be and CAl3Be2â^': global minima with a planar pentacoordinate carbon atom. Chemical Communications, 2010, 46, 8776.	4.1	104
103	Catalytic metal-free ketone hydrogenation: a computational experiment. Dalton Transactions, 2010, 39, 5519.	3.3	38
104	Computational design of metal-free catalysts for catalytic hydrogenation of imines. Dalton Transactions, 2010, 39, 4038.	3.3	45
105	Planar Tetracoordinate Carbon Species Involving Beryllium Substituents. Inorganic Chemistry, 2008, 47, 1332-1336.	4.0	42
106	Water facilitated photolysis of perfluoroalkyl iodides <i>via</i> halogen bonding. Organic Chemistry Frontiers, 0, , .	4.5	6